IEEE Access
Multidisciplinary | Rapid Review | Open Access Journal

Received April 9, 2019, accepted May 10, 2019, date of publication May 28, 2019, date of current version June 18, 2019.

Digital Object Identifier 10.1109/ACCESS.2019.2919579

SIW Multibeam Antenna Array at 30 GHz for 5G Mobile Devices

CARLA DI PAOLA[1], (Student Member, IEEE), KUN ZHAO[1,2], SHUAI ZHANG[1], (Senior Member, IEEE), AND GERT FRØLUND PEDERSEN[1], (Senior Member, IEEE)

[1]Department of Electronic Systems, Antennas, Propagation and mm-Wave Systems (APMS) Section, Aalborg University, 9100 Aalborg, Denmark
[2]Research Center Lund, Sony Corporation, 22188 Lund, Sweden

Corresponding author: Shuai Zhang (sz@es.aau.dk)

This work was supported by the Innovationsfonden Project of Reconfigurable Arrays for Next Generation Efficiency (RANGE).

ABSTRACT This paper presents a new phased array of substrate integrated waveguide (SIW) monopoles, characterized by simple structure, high gain, and large coverage, resulting as a good candidate for next 5G mobile handsets. The design consists of eight monopoles printed on a Rogers RO4003 substrate. In particular, four antennas are located on top of the PCB to cover the area behind the structure and four in the bottom to scan the space in front. Moreover, a high-permittivity dielectric is placed below the elements to stop the surface currents flowing along the ground plane and adjust the beam pointing. The simulations, including three different antenna array combinations, prove that the angle of over 180° can be covered with a peak gain of 12.3 dBi at 30 GHz. The prototype is fabricated, and passive measurements are performed in the anechoic chamber. The results are in accordance with the simulations and confirm the effective benefit given by the dielectric to the radiation performance of the antenna array.

INDEX TERMS Mobile terminal antennas, phased antenna array, multibeam antenna array, high gain, 30 GHz.

I. INTRODUCTION

To meet the increasing demands to achieve higher data rates, the upcoming fifth generation (5G) mobile communication system requires wider bandwidth [1], that supports higher capacity and massive device connectivity and guarantees lower end to-end latency and better user experience. A promising solution is to move up to the millimeter wave bands [2], [3], resulting though in increased free-space path loss, according to the Friis Transmission Equation [4]. However, the large loss can be compensated exploiting higher-gain antennas, but the downsides are narrow radiation beamwidth and consequent reduced coverage. Therefore, as reported in [5], beam-steerable directional phased arrays are adopted to achieve multiple beams and high gain at both the base station and the mobile device in the new 5G systems.

Different antenna array configurations have been investigated in recent years for mm-wave applications. Initially the attention has focused on developing phased array consisting of planar antennas. Quasi-Yagi antennas [6], [7] and printed dipoles [8]–[11], for example, have captured the interest thanks to the features of wide bandwidth and high efficiency, with the disadvantage though of large size.

Later, the advent of the substrate integrated waveguide (SIW) technology [12] allowed to realize components with lower loss and negligible parasitic cross-coupling, making thus the SIW antenna more attractive than conventional planar integrated antenna. For these advantages, SIW technology is considered a suitable candidate for the design of mm-wave antenna, because of simple fabrication, easy integration and low manufacturing cost [13]–[16]. Nevertheless, the dimension and complex configuration represent still a limit in the use of SIW components, as confirmed by the research efforts in [17]–[20].

This paper presents a SIW multibeam antenna array operating at 30 GHz for future 5G mobile devices. Compared with the state-of-the-art prototypes, the design proposed in this paper is characterized by smaller clearance, that allows to optimize the space occupied on the PCB. Eight monopoles are selected as the main radiating elements for the array and, to achieve a low mutual coupling, a microstrip stub is inserted between two adjacent antennas. Three beams with different

The associate editor coordinating the review of this manuscript and approving it for publication was Guan-Long Huang.

TABLE 1. Dimensions of the 5G antennas parameters (Units: mm).

Parameter	Value	Parameter	Value
L_c	3	L_{SIW}	$2\lambda = 20$
L_m	2	W_{SIW}	5.55
W_m	0.4	R_{in}	0.4
W_p	0.5	R_{out}	1

directions can be generated to cover the angle range of around 180° with peak gain of 12.3 dBi, which guarantee high gain over a omnidirectional coverage.

The paper is organized as follows. The design of the structure is described in Section II. Section III presents the analysis conducted on the simulated prototype and deals with the optimization of the radiation performance of the antenna system. Section IV shows the results of the measurements run on the realized component, followed by a comparison with the results obtained from the simulations. Finally, Section V concludes the paper.

II. STRUCTURE OF THE SIW MONOPOLE ANTENNA ARRAY

In the proposed antenna package, shown in Fig. 1, eight monopoles, spaced half wavelength from each other, are printed on both sides of a Rogers RO4003 substrate, with permittivity $\epsilon_r = 3.55$ and loss tangent $\delta = 0.0027$. In particular, the first four monopoles, placed on the top of the PCB, radiate towards the back of the structure ($0° < \phi < 180°$) and the other four, located in the bottom, point their beam to the front ($-180° < \phi < 0°$). Each monopole is fed by a SIW, which plays an important role for the bandwidth and radiation characteristics. The length of the SIW is not a critical parameter, so it is chosen to be 2λ, the minimum distance that guarantees that the *mmpx* connectors are far enough from the monopoles to not affect their radiation pattern. The substrate has length 130 mm, width 70 mm and thickness 1.524 mm. The other dimensions are listed in Table 1. A significant advantage is offered by the short length of the monopoles, which allows to minimize the clearance to 3 mm. Finally, the grounded parallel plates beside adjacent elements aim to reduce the mutual coupling that occurs between them.

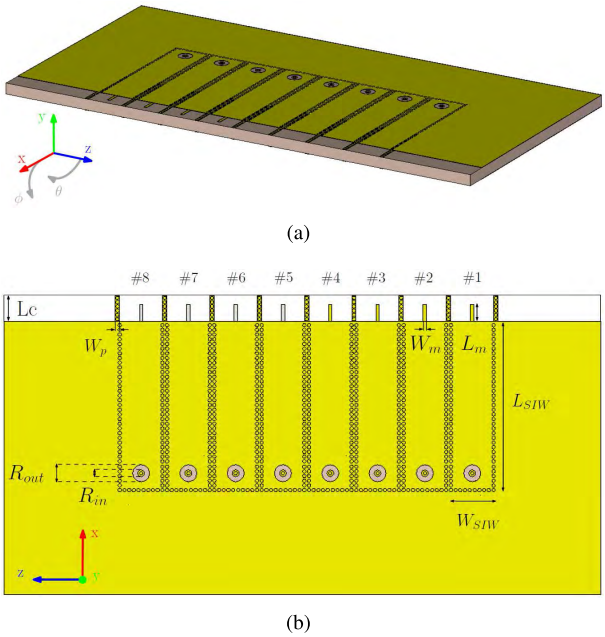

FIGURE 1. (a) Perspective and (b) frontal view of the geometric structure of the proposed SIW monopole antenna array for 5G mobile-phones.

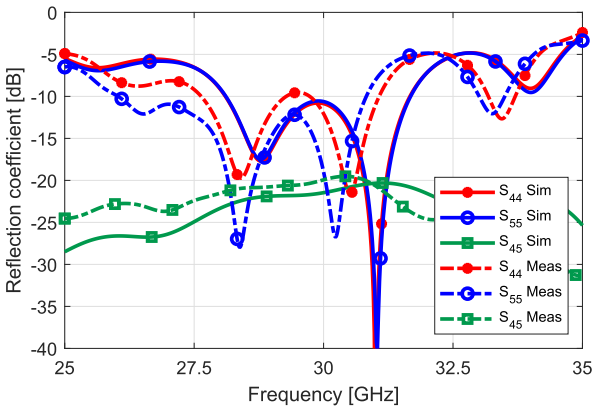

FIGURE 2. Comparison of the simulated and measured S-parameter characteristics of the two middle elements of the proposed antenna package. The reflection coefficient of the other antenna elements closely matches S_{44} and S_{55}.

III. ANTENNAS PERFORMANCE

The structure is analysed using the electromagnetic simulator *CST Microwave Studio 2019*. Since the curves representing the S-parameter characteristics of the array elements are similar, Fig. 2 reports only the ones related to the two middle elements, antenna 4 on the top side of the PCB and antenna 5 in the bottom. The simulated 10 dB bandwidth is $28 - 31$ GHz around the resonant frequency of 30 GHz, which is in inverse proportion to the length of the monopoles. In fact, looking at the results of the parametric simulations carried out over the length of the monopoles and plotted on the graph in Fig. 3(a), it is possible to observe that a reduction of the length increases the return loss, enlarges the bandwidth and moves up the resonance frequency. Same considerations apply to the outcome of the parameterization of the width of the SIW, as shown in Fig. 3(b), where, in addition, the curves highlight that a narrower SIW is responsible for a more evident ripple. Finally, the contribution given by the parallel plates placed beside the monopoles is evaluated and the data are reported in Fig. 4. Whereas the isolation between the neighbouring elements is over 20 dB, when using the plates, removing them means increasing the mutual coupling to -10 dB and loosing the impedance matching, with consequent alteration of the radiation properties. The benefit given by the parallel plates can be verified comparing the flow of the currents generated by antenna 4 in the case without (Fig.5(a)) and with them (Fig.5(b)). In fact, when these are removed, the current is spread along the short edge of the ground plane to the

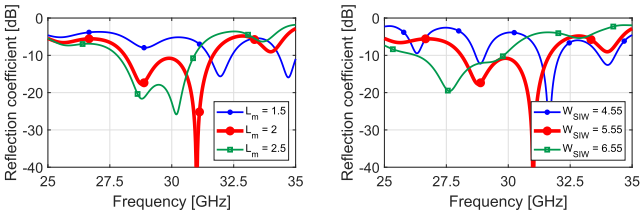

FIGURE 3. Simulated S-parameter characteristics of the first antenna element varying (a) the length L_m of the monopole and (b) the width W_{SIW} of the SIW.

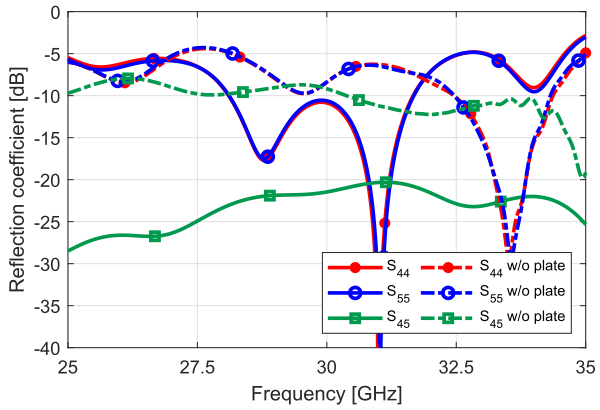

FIGURE 4. Simulated S-parameter characteristics of antenna 4 and 5, when the parallel plates are removed.

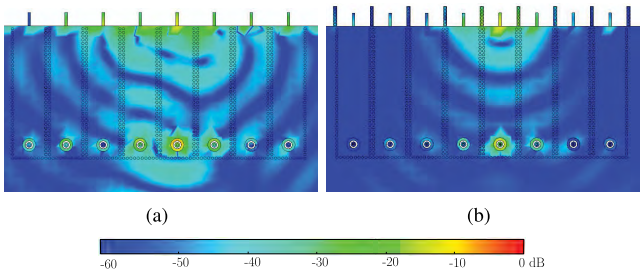

FIGURE 5. Coupled current on the neighbouring elements, when port 4 is excited, in the configuration (a) without and (b) with the parallel plates.

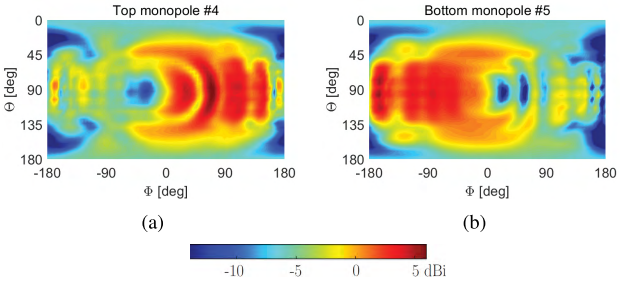

FIGURE 6. Simulated 3D-radiation patterns of (a) antenna 4 on top and (b) antenna 5 in the bottom at 30 GHz. For ϕ varying from 0° to 360° the corresponding value along θ has been plotted.

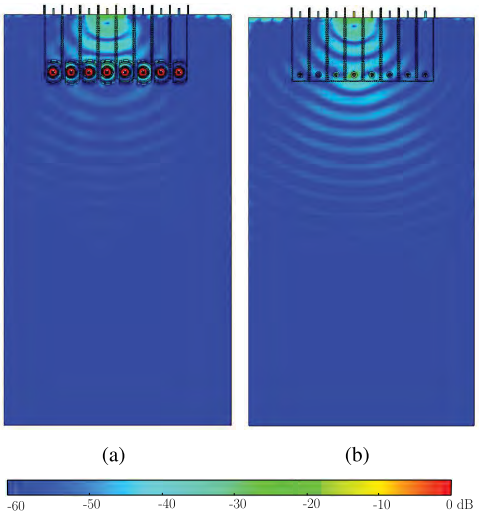

FIGURE 7. Surface currents generated by (a) antenna 4 and (b) antenna 5.

neighbouring elements. In addition, the mutual coupling is particularly visible looking at the effects on the connectors beside that of the radiating element and to a small extent also on the other elements. On the other hand, exploiting the parallel plates, the current generated by antenna 4 has minor influence on antennas 3 and 5 and negligible effect on the others.

Figure 6 shows the 3D radiation characteristic of the reference antennas at 30 GHz. As expected, antenna 4 on top radiates towards the direction ($0° < \phi < 180°$), whereas antenna 5 in the bottom scans the portion of area where ($-180° < \phi < 0°$). However, looking at Fig. 6(a), apart from the main beam pointing at $\phi = 60°$ with a realized gain of 6 dBi, significant components are visible also where $\phi < 150°$. The same applies to antenna 5 in Fig. 6(b) but, in this case, the main beam is directed down, while the desired area is covered with approximately 3 dBi.

Therefore, in order to investigate the source of this unwanted radiation, the surface currents related to the reference antenna elements are calculated and reported in Fig. 7. In both cases, it is evident that the current generated by the antenna flows down along the ground plane. However, considering antenna 4 in Fig. 7(a), the presence of the connectors limits the current strength, which results reduced compared to antenna 5 in Fig. 7(b).

A. HIGH PERMITTIVITY DIELECTRIC TO BLOCK THE SURFACE CURRENTS

The aim of the proposed solution is to place a high permittivity dielectric below the monopoles on both sides of the PCB, as shown in Fig. 8, with the function to absorb the current flow radiated by the antenna elements. The substrate chosen for this purpose is Duroid 6010, with dielectric constant $\epsilon_r = 10.2$, $Lp = 3$ mm long and $Tp = 1.24$ mm thick, with a metalization $Ls = 0.5$ mm long on top, grounded in the antenna ground plane. The new component does not affect the impedance matching.

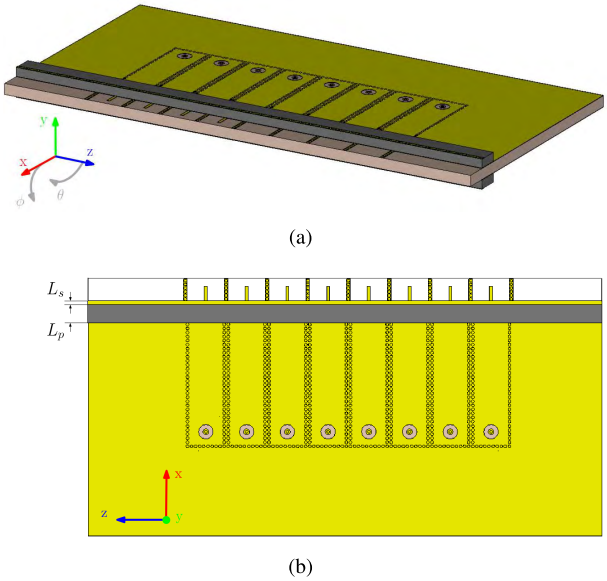

FIGURE 8. (a) Perspective and (b) frontal layout of the proposed SIW monopole antenna array with high permittivity dielectric placed below the monopoles.

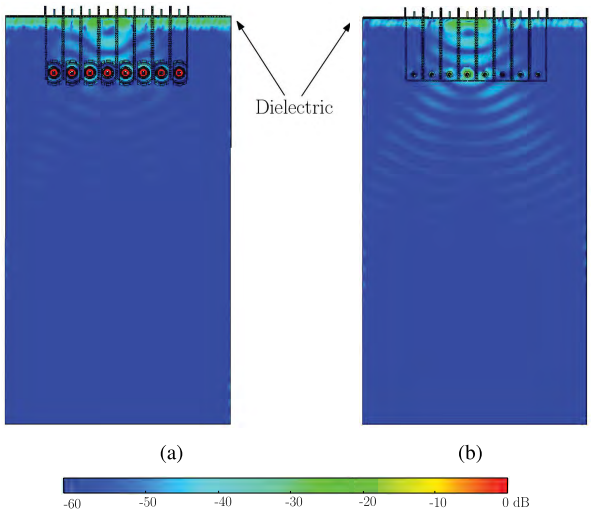

FIGURE 9. Effects of the high permittivity dielectric on the surface currents propagation. Currents generated by (a) antenna 4 and (b) antenna 5.

As depicted in Fig. 9, most of the current generated by the two reference antennas is spread along the dielectric and only a minor part flows down through the surface of the ground plane. The benefit obtained can also be seen after comparison with the previous Fig. 7. With the solution adopted, the realized gain of each array element increases of 1 dB, compared to the original case. Moreover, a broader coverage with a scanning angle wider than 60° is guaranteed by both antennas. In particular, the radiation patterns result almost symmetric and, above all, cover only the desired part of the space, as Fig. 10 proves.

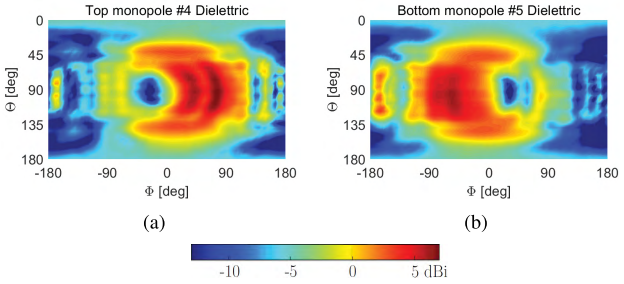

FIGURE 10. Simulated 3D-radiation patterns of (a) antenna 4 on top and (b) antenna 5 in the bottom at 30 GHz, when the high permittivity dielectric is placed on both sides of the PCB. For ϕ varying from 0° to 360° the corresponding value along θ has been plotted.

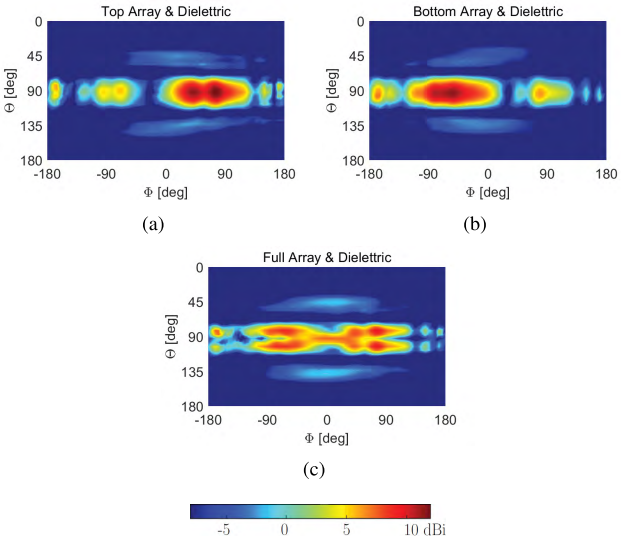

FIGURE 11. Simulated 3D-radiation patterns at 30 GHz of (a) phased array made up of the 4 antenna elements on top, (b) phased array made up of the 4 antenna elements in the bottom and (c) phased array made up of the 8 antenna elements, when the high permittivity dielectric is placed on both sides of the PCB. For ϕ varying from 0° to 360° the corresponding value along θ has been plotted.

B. PHASED ARRAY OF SIW MONOPOLE ANTENNAS

In order to cover the area of 180° with high gain, three different phased array are required. The first is made up of the four monopoles on top (antennas $1-4$ in Fig. 1) combined with phase shift $\alpha = 0°$ and scans the space in front of the antenna. The second consists of the four elements in the bottom (antennas $5-8$) and points to the back. Finally, to guarantee the desired coverage above the structure, all the antennas are exploited.

Comparing the radiation pattern related to the top and bottom arrays, represented in Figs. 11(a) and 11(b) respectively, with that generated by the corresponding antenna element in Fig. 10, a significant reduction of the beamwidth along θ from 70° to 20° can be observed, which allows to achieve higher gain, as expected.

The 2D-coverage property of the antenna system at 30 GHz is reproduced in Fig. 12(b). The curve representing the

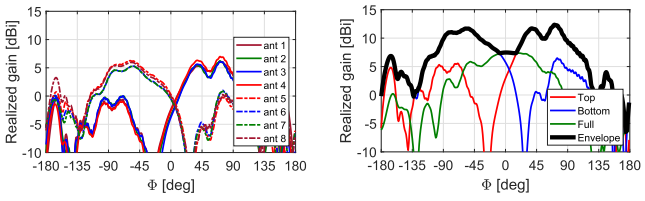

(a) (b)

FIGURE 12. Comparison of the spherical coverage at 30 GHz of (a) every single monopole and (b) the phased arrays obtained by three different combinations of the antenna elements with phase shift $\alpha = 0°$.

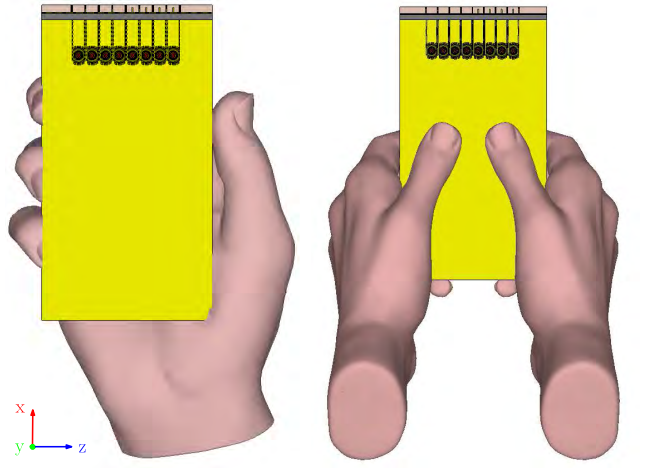

(a) (b)

FIGURE 13. Simulations including (a) right hand and (b) double hand to evaluate the user influence on the efficiency and radiation performance of the SIW monopole antenna array.

envelope shows that it is possible to steer the beam from −100° to 100° with a gain higher than 7 dBi. In particular, the eight elements array covers an area of 20° with maximum gain of 7.5 dBi at 0°, whereas the top and bottom array scan each 90° with peak gain of 12.3 and 11.7 dBi respectively at 70° and −60°. Moreover, the curves representing the coverage of the top and bottom arrays have the same trend as the corresponding single elements in Fig. 12(a)), but show a realized gain 6 dB higher.

In Table 2 the proposed design is compared with previous studies on SIW antenna array both in terms of structural characteristics and based on key performance metrics. It turns out that, due to the small clearance occupied by the radiating elements and the wide coverage achieved with high gain, the SIW monopole antenna array represents a good trade-off between dimensions and performance.

C. INVESTIGATION OF THE USER IMPACT

The investigation of the user influence on the radiation performance of the proposed SIW monopole antenna array, with and without the high permittivity dielectric, is carried out through simulations in data mode considering the right hand and both hands, as represented in Fig. 13(a) and Fig. 13(b)

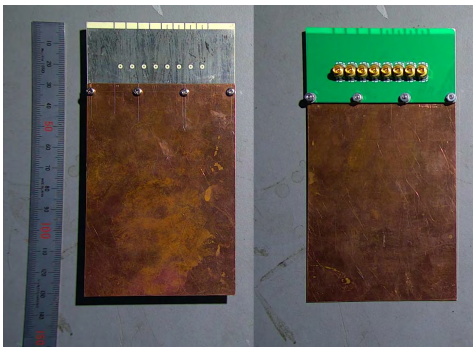

(a)

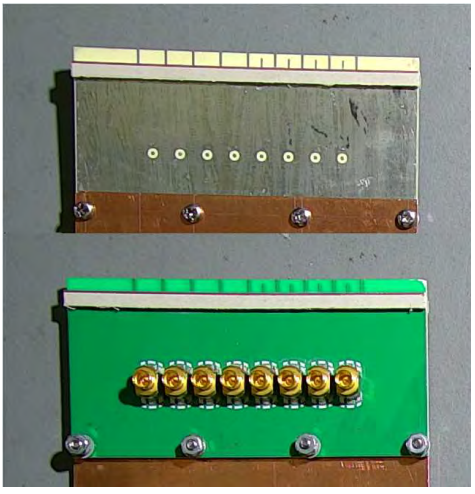

(b)

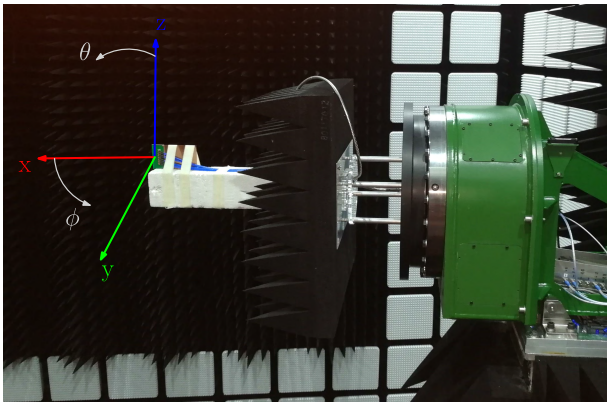

(c)

FIGURE 14. (a) Fabricated SIW monopole antenna array on a Rogers RO4003 substrate (top and bottom layer), (b) with high permittivity stick glued on top and bottom and (c) measurements setup in the anechoic chamber.

respectively. Considering the antenna only, the results show that the single hand has the same effect as adding the high permittivity dielectric, i.e. blockage of the flow of the surface currents towards the bottom of the PCB. However, the presence of the hand causes a reduction of 1.5 dB in efficiency, which is more significant when the structure is hold with two hands. On the other hand, the total efficiency of the antenna with the high permittivity dielectric is not altered by the hand,

TABLE 2. Comparison of the proposed design with previous work.

Parameters	Proposed design	[15]	[16]	[19]	[20]
Total area (mm^2)	23×49	34×20	30×28	48×55	150×54
Clearance (mm)	3	14	0	0	0
N° antennas	8	4	16	11	14
Bandwidth (GHz)	$28 - 31$	$32.5 - 35$	$41 - 45$	$28.2 - 31.5$	$33 - 37$
Center frequency (GHz)	30	33.5	42	30	35
Peak gain (dBi)	12.3	9.7	17.3	20.2	18.9
Coverage azimuth elevation	 110° 200°	 76° –	 25.4° 16.3°	 118° –	 38° 86.6°

which decreases though the gain of the three beams of 1 dB on average. Negligible effect is given instead by the two hands.

IV. MEASUREMENTS RESULTS AND DISCUSSION

Figure 14(a) shows the fabricated SIW monopole antenna array prototype. The S-parameter characteristics of the two reference elements, evaluated with the Keysight N5227A Power Network Analyzer (PNA) are reported in Fig. 2. The trend of the simulated and experimental return loss curves matches each other and the bandwidth is confirmed to be 3.5 GHz. Nevertheless, the resonance frequency of the realized component is shifted 500 MHz backward, possibly due to the longer length of the printed monopoles, as proved by the parametric study in Fig. 3(a). The shift in frequency is visible also comparing the curves representing the mutual coupling between the two ports. However, the measured isolation, higher than 20 dB over the whole bandwidth, confirms the effective benefit given by the metal plates beside the monopoles.

The radiation performance of the realized component are measured in the anechoic chamber located at the Antenna, Propagation and mm-Wave Systems (APMS) section at Aalborg University. In Fig. 14(c) the antenna under test (AUT) is suitably positioned on the measurements setup. The test equipment consists of a dual polarized test probe, which allows to evaluate the gain at each selected point over the ϕ-axis, when $\theta = 90°$. The power is recorded for the test probe for both polarizations and the procedure is repeated until the interval $-135° < \phi < 135°$ is measured, rotating the AUT by 5 degrees per time. The choice of ϕ is justified by the dimension of the setup, that would be placed between the test probe and the AUT, compromising thus the results. The measurements are carried out in the frequency interval $26 - 35$ GHz.

The 2D-coverage properties of the simulated and realized antenna 4 and 5 at 30 GHz are reported in Figs. 15(a) and 15(c) respectively. From the comparison of the curves, it is possible to state that the measured results closely match the simulations and the expected beam steering is obtained. However, it is possible to notice a decrease in gain of 2 dB on average, caused by the different impedance matching between the simulated and realized prototype.

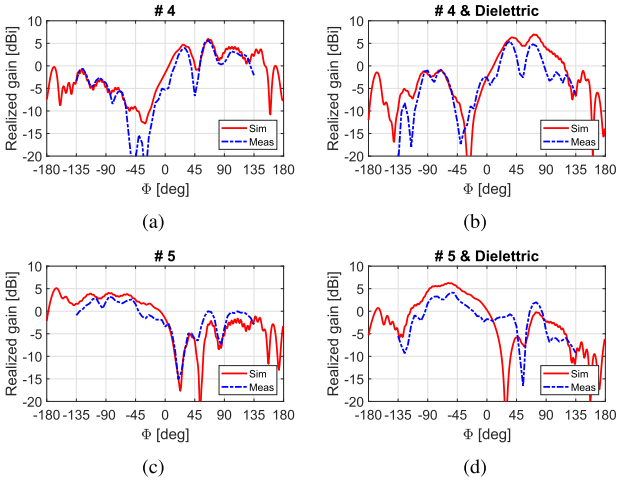

FIGURE 15. 2D-radiation pattern at 30 GHz for the reference antenna (a) 4 and (c) 5 and impact of the dielectric mounted on both sides of the substrate on the radiation performance of antenna (b) 4 and (d) 5. For ϕ varying from $-135°$ to 135° the corresponding realized gain has been plotted for both simulations and measurements.

Moreover, to investigate the effective impact of the dielectric on the radiation performance, two pieces of Duroid 6010, with the same design characteristics as in the simulations, are glued on both sides of the PCB, as shown in Fig. 14(b). In this case, looking at the curves of the reference elements in Figs. 15(b) and 15(d), it is possible to notice a more significant decrease in gain of the measured structure compared to the simulated one. In fact, the reduction is approximately 3 dB and can be ascribed to the actual positioning of the dielectric and the contribution of the glue. However, the main objective is achieved, the surface currents are blocked and it is possible to observe that the gain drops when $\phi > 90°$ for antenna 4 and $\phi < -90°$ for antenna 5.

V. CONCLUSION

This work proposes a new antenna array for the upcoming 5G mobile communication systems. The design consists of eight SIW monopoles, suitably placed on both sides of the short edge of the mobile device PCB. The radiation performances are optimized exploiting a high permittivity dielectric below the antenna elements, that reduces the impact of the surface currents and allows to achieve the desired beam pointing.

Moreover, three arrays obtained by different combinations of the monopoles scan an area wider than 180°, with peak gain of 12.3 dBi at 30 GHz. The structure is fabricated and then measured in the anechoic chamber. The results are evaluated in terms of 2D-radiation pattern of the single elements, with particular focus on the contribution of the high permittivity substrate. The radiation properties of the realized prototypes and the benefits given by the dielectric are confirmed, despite a reduction in gain of 2 and 3 dB is measured for the original and enhanced structure respectively. Future work aims to improve the proposed design, in order to realize a wide beam scanning also along theta and obtain 3D-coverage.

ACKNOWLEDGMENTS

The authors would like to thank lab engineers Ben Krøyer, for valuable guidance in the realization of the prototype, Kristian Bank and Kim Olesen, for precious assistance in the measurements setup. The work presented in this paper has been conducted under the framework of the RANGE project, supported by The Innovation Fund Denmark together with industry partners: WiSpry, AAC and Sony Mobile.

REFERENCES

[1] J. G. Andrews, S. Buzzi, W. Choi, S. V. Hanly, A. Lozano, A. C. K. Soong, and J. C. Zhang, "What will 5G be?" *IEEE J. Sel. Areas Commun.*, vol. 32, no. 6, pp. 1065–1082, Jun. 2014.

[2] T. S. Rappaport, S. Sun, R. Mayzus, H. Zhao, Y. Azar, K. Wang, G. N. Wong, J. K. Schulz, M. Samimi, and F. Gutierrez, "Millimeter wave mobile communications for 5G cellular: It will work!" *IEEE Access*, vol. 1, pp. 335–349, May 2013.

[3] T. Bai and R. W. Heath, Jr., "Coverage and rate analysis for millimeter-wave cellular networks," *IEEE Trans. Wireless Commun.*, vol. 14, no. 2, pp. 1100–1114, Feb. 2014.

[4] C. A. Balanis, *Antenna Theory: Analysis and Design*. Hoboken, NJ, USA: Wiley, 2016.

[5] W. Hong, K.-H. Baek, Y. Lee, Y. Kim, and S.-T. Ko, "Study and prototyping of practically large-scale mmWave antenna systems for 5G cellular devices," *IEEE Commun. Mag.*, vol. 52, no. 9, pp. 63–69, Sep. 2014.

[6] W. R. Deal, N. Kaneda, J. Sor, Y. Qian, and T. Itoh, "A new quasi-Yagi antenna for planar active antenna arrays," *IEEE Trans. Microw. Theory Techn.*, vol. 48, no. 6, pp. 910–918, Jun. 2000.

[7] R. A. Alhalabi and G. M. Rebeiz, "High-gain Yagi-Uda antennas for millimeter-wave switched-beam systems," *IEEE Trans. Antennas Propag.*, vol. 57, no. 11, pp. 3672–3676, Nov. 2009.

[8] Y.-H. Suh and K. Chang, "A new millimeter-wave printed dipole phased array antenna using microstrip-fed coplanar stripline tee junctions," *IEEE Trans. Antennas Propag.*, vol. 52, no. 8, pp. 2019–2026, Aug. 2004.

[9] S. X. Ta, H. Choo, and I. Park, "Broadband printed-dipole antenna and its arrays for 5G applications," *IEEE Antennas Wireless Propag. Lett.*, vol. 16, pp. 2183–2186, 2017.

[10] B. Edward, "A broadband printed dipole with integrated balun," *Microw. J.*, pp. 339–344, May 1987.

[11] Q.-Q. He, B.-Z. Wang, and J. He, "Wideband and dual-band design of a printed dipole antenna," *IEEE Antennas Wireless Propag. Lett.*, vol. 7, pp. 1–4, 2008.

[12] D. Deslandes and K. Wu, "Integrated microstrip and rectangular waveguide in planar form," *IEEE Microw. Wireless Compon. Lett.*, vol. 11, no. 2, pp. 68–70, Feb. 2001.

[13] W. Hong, "Development of microwave antennas, components and subsystems based on SIW technology," in *Proc. IEEE Int. Symp. Microw., Antenna, Propag. EMC Technol. Wireless Commun.*, vol. 1, Aug. 2005, p. P-14.

[14] K. Wu, Y. J. Cheng, T. Djerafi, X. P. Chen, N. Fonseca, and W. Hong, "Millimeter-wave integrated waveguide antenna arrays and beamforming networks for low-cost satellite and mobile systems," in *Proc. 4th Eur. Conf. Antennas Propag.*, Apr. 2010, pp. 1–5.

[15] Y. J. Cheng and Y. Fan, "Millimeter-wave miniaturized substrate integrated multibeam antenna," *IEEE Trans. Antennas Propag.*, vol. 59, no. 12, pp. 4840–4844, Dec. 2011.

[16] T. Y. Yang, W. Hong, and Y. Zhang, "Wideband millimeter-wave substrate integrated waveguide cavity-backed rectangular patch antenna," *IEEE Antennas Wireless Propag. Lett.*, vol. 13, pp. 205–208, 2014.

[17] S.-I. Yamamoto, J. Hirokawa, and M. Ando, "A beam switching slot array with a 4-way butler matrix installed in single layer post-wall waveguides," *IEICE Trans. Commun.*, vol. 86, no. 5, pp. 1653–1659, May 2003.

[18] E. Sbarra, L. Marcaccioli, R. V. Gatti, and R. Sorrentino, "A novel rotman lens in SIW technology," in *Proc. Eur. Radar Conf.*, Oct. 2007, pp. 236–239.

[19] Y. J. Cheng, W. Hong, and K. Wu, "Design of a substrate integrated waveguide modified R-KR lens for millimetre-wave application," *IET Microw., Antennas Propag.*, vol. 4, no. 4, pp. 484–491, Apr. 2010.

[20] Y. J. Cheng, W. Hong, K. Wu, and Y. Fan, "Millimeter-wave substrate integrated waveguide long slot leaky-wave antennas and two-dimensional multibeam applications," *IEEE Trans. Antennas Propag.*, vol. 59, no. 1, pp. 40–47, Jan. 2011.

CARLA DI PAOLA received the bachelor's and master's degrees in telecommunication engineering from the University of Catania, Italy, in 2013 and 2016, respectively. She is currently a Ph.D. Fellow with the Department of Electronic Systems, Antennas, Propagation and Millimeter-Wave Systems Section, Aalborg University, Denmark. Her current research interests include antenna design for mobile phones and OTA testing.

KUN ZHAO received the B.S. degree in communication engineering from the Beijing University of Posts and Telecommunications (BUPT), Beijing, China, in 2010, the M.S. degree in wireless systems, and the Ph.D. degree in electromagnetic engineering from the Royal Institute of Technology (KTH), Stockholm, Sweden, in 2012 and 2017, respectively. He was a Visiting Researcher with the Department of Electrical and Information Technology, Lund University, Sweden. He is currently a Researcher of antenna technology and standardization with the Radio Access Laboratory, Sony Mobile Communication AB, Lund, Sweden. He is also an Industrial Postdoctoral with Aalborg University, Denmark. His current research interests include mm-wave antenna and propagation for 5G communications, MIMO antenna systems, user body interactions, and body centric wireless communications.

SHUAI ZHANG (SM'18) received the B.E. degree from the University of Electronic Science and Technology of China, Chengdu, China, in 2007, and the Ph.D. degree in electromagnetic engineering from the Royal Institute of Technology (KTH), Stockholm, Sweden, in 2013. He was a Research Fellow with KTH. From 2010 to 2011, he was a Visiting Researcher with Lund University, Sweden, and also with Sony Mobile Communications AB, Sweden. In 2014, he joined Aalborg University, Denmark, where he is currently an Associate Professor. He was also an External Antenna Specialist with Bang & Olufsen, Denmark, from 2016 to 2017. He has coauthored over 60 articles in well-reputed international journals, and he holds over 16 US or WO patents. His current research interests include mobile terminal mm-wave antennas, biological effects, cubesat antennas, massive MIMO antenna arrays, UWB wind turbine blade deflection sensing, and RFID antennas.

GERT FRØLUND PEDERSEN was born in 1965. He received the B.Sc.E.E. degree (Hons.) in electrical engineering from the College of Technology, Dublin Institute of Technology, Dublin, Ireland, in 1991, and the M.Sc.E.E. and Ph.D. degrees from Aalborg University, Aalborg, Denmark, in 1993 and 2003, respectively.

He was a Consultant for the development of more than 100 antennas for mobile terminals, including the first internal antenna for mobile phones, in 1994, with lowest SAR, first internal triple-band antenna, in 1998, with low SAR, high TRP, and TIS, and, lately, various multiantenna systems rated as the most efficient on the market. Most of the time, he was with joint university and industry projects and has received more than 21 M$ in direct research funding. Since 1993, he has been with Aalborg University, where he is currently a Full Professor heading the Antennas, Propagation and Millimeter-wave Systems Laboratory with 25 researchers. He is also the Head of the Doctoral School on wireless communication with some 40 Ph.D. students enrolled. He is also the Project Leader of the Range Project with a total budget of over eight M$ investigating high performance centimeter-/millimeter-wave antennas for 5G mobile phones. He has published more than 500 peer-reviewed papers, six books, and 12 book chapters. He holds over 50 patents. His research interests include radio communication for mobile terminals, especially small antennas, diversity systems, propagation, and biological effects. He is also involved in MIMO OTA measurement. He has been one of the pioneers in establishing over-the-air measurement systems. The measurement technique is now well established for mobile terminals with single antennas, and he was the Chair of the various COST groups with liaison to 3GPP and CTIA for over-the-air test of MIMO terminals.